Rotor Yoke Effect on Core Losses of a Non-Overlap Wound-Rotor Synchronous Machine

K. S. Garner and M. J. Kamper

***Abstract* – The focus of the paper is on the reduction of core losses of large wound-rotor synchronous machines with non-overlap stator windings. The wound-rotor synchronous machine, being one of the alternatives to the permanent magnet synchronous machine, has the important advantage that the rotor field flux can be varied. The use of non-overlap stator windings is growing due to the associated improved torque density and simpler manufacturing, but at the expense of a higher harmonic content in the magnetomotive force distribution. The latter causes the core losses in wound-rotor synchronous machines to increase. This paper shows that the rotor yoke design has an important effect on these losses. Rotor yoke design strategies are applied in the paper to limit the amount of harmonic flux setup in the rotor core. Flux barriers in the rotor yoke are deemed to have the overall best effect on the machine performance by reducing the rotor core losses while not increasing torque ripple and maintaining output power.**

***Index Terms*—core loss, flux barrier, harmonic, non-overlap, saturation, wound-rotor, synchronous machine, yoke**

I. INTRODUCTION

Constrained electricity supply is one of the driving factors to develop more energy-efficient machines. This requires looking critically at reducing machine losses, particularly in large machines where these losses become significant. Electric machine losses are categorised into mechanical losses, winding losses and core losses. The research around mechanical and winding losses of electric machines is extensive, but core losses are not as easily modelled. These losses are the result of the fluctuating magnetic field in the stator and rotor cores and are dependent on the material type and the amount of flux travelling through the material [1].

Core losses are further compounded with the use of non-overlap stator windings. Non-overlap stator windings are becoming more prevalent in electric machine designs in the place of traditional overlap stator windings. The popularity of overlap stator windings stems from the low harmonic content in the produced magnetomotive force (MMF), which in turn translates into better machine performance. Nonetheless, the winding arrangement is more complex and the relatively long end windings increase the conduction losses. Some improvements offered by the application of non-overlap windings are, although not limited to, higher torque density, reduction in copper required, simpler manufacturing and lower cogging torque [2]. The considerable drawback is the high amount of sub-harmonic content in the MMF waveform that manifests as increased core losses in the rotor [2]. These windings have been used mostly in permanent magnet (PM) machines, but more studies are now looking at the implications of applying the winding structure to other electric machines.

Although core losses are applicable to both the stator and rotor, only the rotor core losses are investigated in this paper. The core loss reduction approach presented in this study is applied to a large wound-rotor synchronous machine. Wound-rotor synchronous machines (WRSMs) are being considered as an alternative solution to permanent magnet synchronous machines, particularly because of their lack of permanent magnetic material and their important ability to vary the rotor field flux. The latter is important for flux weakening in the high-speed region of variable speed drives and for the reactive power control of direct grid-connected machines.

This study looks at the rotor yoke design in an effort to reduce the rotor core losses of the WRSM by (i) the application of flux barriers in the rotor yoke, (ii) reducing the thickness of the rotor yoke and (iii) applying a non-uniform rotor yoke. The model in question is a 3 MW, WRSM with a 16/18 pole/slot combination and a non-overlap stator winding using a phase-shifting technique of [3]. The results of [3] show that many of the sub- and higher order harmonics of a non-overlap stator winding can be reduced and in turn improve the torque and power density of the machine. However, it is shown that the rotor core losses increase with the use of non-overlap stator windings. A method is proposed in [3] to reduce the rotor core losses, which this study aims to investigate further in greater detail. Flux barriers are used in synchronous reluctance and permanent magnet machines to facilitate generating torque. The positioning and shape of the barriers are shown to affect torque ripple and core losses [5], [11] , [12]. The inclusion of flux barriers limits the amount of harmonic flux traveling through the rotor core, thereby reducing the rotor core losses.

The effect of the thickness of the rotor yoke is investigated as an alternative to the rotor yoke flux barriers. It is well known that the rotor yoke thickness plays an important role in the generated wound-field flux and thus in the performance of the machine. Hence, the accompanying average torque, torque ripple and rotor core losses are of interest in the comparison study. The third element of the study investigates a hybrid of the flux barriers and the reduced rotor yoke by means of a non-uniform rotor yoke. Again, the machine performance is compared.

The study is conducted by way of 2-D finite element analysis (FEA) using models constructed in ANSYS Max-

K. S. Garner acknowledges the financial support of the NRF, South Africa.

K. S. Garner and M. J. Kamper are with the Department of Electrical and Electronic Engineering, Stellenbosch University, Stellenbosch, 7600, South Africa (e-mails: garnerks@sun.ac.za; kamper@sun.ac.za).

978-1-7281-9944-3/20/$31.00 ©2020 IEEE

well. Only the rotor yoke dimensions are varied in the study, while keeping the stator and applied stator current constant.

II. Machine Specifications

A cross-section of the machine considered in this paper is displayed in Fig. 1 and Table I details the specifications of the WRSM considered in the paper. The machine has 16 rotor poles and 18 stator slots, with a double layer, phase-shifted, non-overlapping winding of [3]. Fig. 2 displays the resulting MMF harmonic distribution of this stator winding. The base value of the per unit calculation is the working harmonic of the conventional non-overlap winding. The working 4^{th} MMF harmonic is strengthened with the phase-shifted winding, but so too is the 5^{th} MMF harmonic, while the sub- and higher-order MMF harmonics are considerably reduced. It is the large 5^{th} MMF harmonic in Fig. 2 that increases the rotor core losses. In Fig. 3, the full-load output torque waveform of the 3 MW machine with only q-axis stator current is shown. This shows a torque ripple of about 9.5 %.

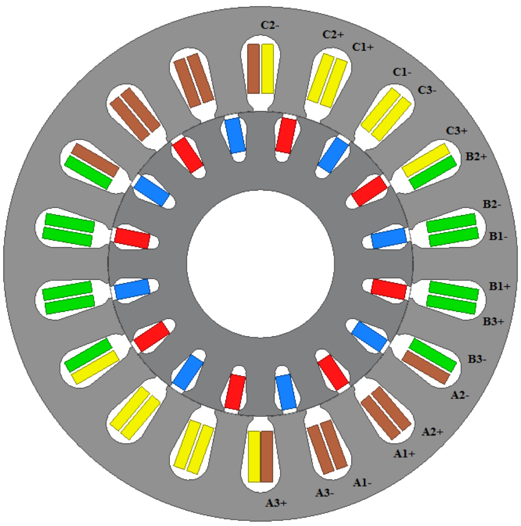

Fig. 1. Cross-section and winding layout of the phase-shifted 16/18 pole-slot WRSM [3].

TABLE I: DESIGN SPECIFICATIONS OF 3 MW WRSM.

Specifications	Numerical value
Rated power [MW]	3
Rated torque [kNm]	76
Rated speed [r/min]	375
Rated frequency [Hz]	50
Number of poles	16
Number of stator slots	18
Stator outer diameter [mm]	1600
Rotor outer diameter [mm]	947
Rotor inner diameter [mm]	460
Stack length [mm]	1500
Air gap length [mm]	1.5
Efficiency [%]	97.55
Stator core loss [kW]	23.19
Rotor core loss [kW]	8.84

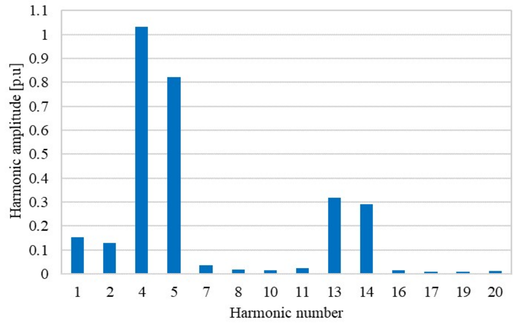

Fig. 2. MMF harmonic distribution of phase-shifted non-overlapping winding WRSM [3].

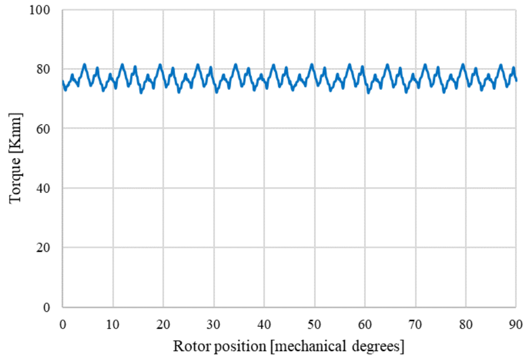

Fig. 3. Calculated torque and torque ripple of the WRSM [3].

Core losses are a function of the type of material, the amount of flux penetrating the material and the frequency of the flux variation. International standards, such as the IEC 60404-1 [6], exist that describe the magnetic properties of materials for electric machines. Manufacturers provide loss ratings for their materials at a per-mass rating for a peak flux density. This means that there are different loss ratings for different flux densities penetrating the same material. In core loss analysis the machine is therefore divided into n sections based on the flux density. The core loss for a section at a certain frequency can be described by [1]

$$P_{Fe,n} = P_{15}\left(\frac{B_n}{1.5}\right)^2 m_{Fe,n}\,, \tag{1}$$

where P_{15} is the loss rating of the material for a peak flux density of 1.5 T, B_n is the peak flux density of the section and $m_{Fe,n}$ is the corresponding mass of the section.

Existing methods of core loss reduction rely mostly on motor design optimization and pole-slot number combinations [7] - [10]. It is evident from (1) that to reduce the core loss, the mass, material loss rating and/or the peak flux density must be reduced. The mass and material loss ratings are difficult parameters to modify because they are directly related to the material available and the iterative process of the machine design. Lowering the peak flux density in a section can be achieved if the amount of peak flux variation can be inhibited. Special flux barrier shaping of an interior PM-rotor synchronous machine has shown to reduce rotor core losses significantly [11]. The aim in the paper is to place flux barriers in the rotor core yoke as a means of reducing the harmonic travelling fluxes in the rotor core.

III. Flux Barrier Design Strategy

The shape and positioning of flux barriers in the core will influence the magnetic flux in both the direct and quadrature directions. Considering the natural flow of the magnetic flux in the machine, it would seem prudent to allow the flux barriers to mimic this flow to channel flux away from the inner yoke core towards the rotor teeth. This is also the main design consideration for the shape of flux barriers in reluctance and permanent magnet machines [5], [11], [12]. Fig. 4 displays the basic design of the rotor yoke flux barrier. The thickness and position of the barriers are varied to minimise the rotor core loss, with sufficient iron maintained between the barrier-ends for structural rotor integrity.

A. *Variation in Barrier Thickness*

Fig. 5 depicts the workflow used for the variation of the flux barrier thickness. The basic flux barrier is placed halfway between the innermost point of the rotor slot and the shaft as depicted in Fig. 6(a). This is done to create a baseline for the variation of the thickness of the barrier. The study looked at determining the optimum position first and then the thickness, but it was found that the order of the variations did not affect the final resulting barrier design. Fig. 6(b) shows the flux barrier with a 20 mm thickness at its largest section. The barriers are tapered due to the space constraint between the barriers. The study capped the thickness to 20 mm to prevent the inner yoke iron below the barrier from becoming too thin and creating a structural concern.

Table II displays some key points of the Maxwell FEA predicted machine performance at rated q-axis stator current versus barrier thickness variation. Though the rotor core losses decrease with an increased flux barrier thickness, it is at the cost of a slight increased torque ripple and decreased average torque. The flux barriers in the rotor core are able to limit flux travelling through the inner core of the rotor, but some flux around the teeth of the rotor is also inhibited when the barrier becomes too large. The slight decrease in average torque with a very large barrier can be attributed to the slight drop in rotor field flux.

Fig. 7 shows graphically the effect of the variation of the barrier thickness on the torque ripple and rotor core losses. The 5 mm flux barrier thickness is selected as the optimum value thickness in terms of average torque, torque ripple and rotor losses.

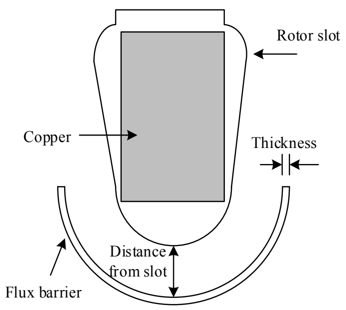

Fig. 4. Basic design shape of the rotor yoke flux barrier.

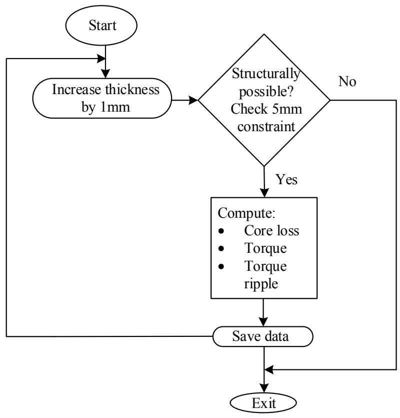

Fig. 5. Workflow strategy of the variation of the barrier thickness.

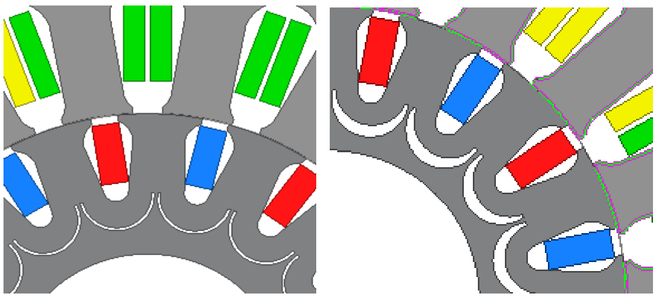

(a) (b)

Fig. 6. FE models depicting (a) baseline 5 mm flux barrier position and (b) 20 mm rotor yoke flux barriers.

TABLE II: PERFORMANCE OUTPUT OF VARIATION OF FLUX BARRIER THICKNESS.

Performance parameter	No barrier	1 mm	5 mm	10 mm	20 mm
Power [MW]	3.05	3.03	3.04	3.02	3.00
Average torque [kNm]	77.58	77.26	77.5	77.13	76.36
Torque ripple [%]	9.53	9.53	9.53	9.82	10.76
Rotor core loss [kW]	8.84	6.87	4.9	4.75	4.5
Stator core loss [kW]	23.19	23.19	23.17	23.17	23.18
Efficiency [%]	97.6	97.60	97.67	97.66	97.65

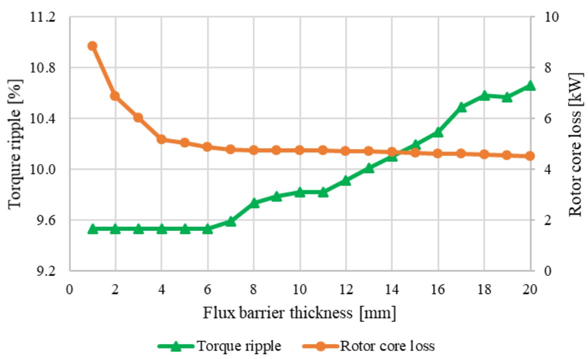

Fig. 7. Effect of the flux barrier thickness on the torque ripple and rotor core losses.

B. Variation in Barrier Position

With the thickness of the barrier set at its optimum value of 5 mm, the optimum position can be determined. The positioning of the flux barriers also plays a significant role in the core loss reduction. If the barrier is too close to the slot, the flux cannot travel around the teeth; too far and the barriers do not prevent enough flux travelling through the rotor yoke. Another constraint is the distance from the barrier to the inner rotor diameter, which could negatively influence the structural integrity of the rotor. The workflow of the variation of the position of the flux barrier is displayed in Fig. 8. The barrier was moved by 5 mm in each iteration. The 5 mm constraint between the barriers was maintained.

The results in Fig. 9 show that the most efficient placement of the barriers for this machine is at 45 mm, which is also half the width of the rotor tooth. The furthest the barrier could be placed within the constraints was 70 mm.

IV. Flux Density Analysis

The results of the previous section show that the flux barriers can limit the rotor core losses when a machine has a large rotor yoke if the correct placement and thickness is selected. It is prudent to observe the flux density in the air gap, around the teeth and around the flux barriers to assist in verifying the effect of the barriers.

A. Air gap Flux Density Variation

Fig. 10 depicts the air gap flux density without and with barriers. Not much difference is noted between the two waveforms, but the main difference can be seen during the transition from one slot to the next. In Fig. 11, the amplitude variation of the 5th harmonic air gap flux density versus rotor position is shown. There is a relatively large suppression of this harmonic flux density by the rotor yoke barriers, which gives a first explanation of the reduced rotor core losses as expected from (1). A further harmonic analysis of the air gap flux density is depicted in Figs. 12 – 14. Three scenarios are created: (i) no phase current and rated field current in Fig. 12 that is used as the base value for the comparison, (ii) rated phase current and no field current in Fig. 13 and (iii) rated phase current and rated field current in Fig. 14. It is noted throughout the three scenarios that the inclusion of yoke flux barriers reduces the effect of the 5th harmonic specifically.

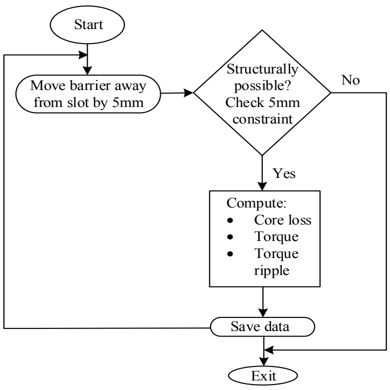

Fig. 8. Workflow strategy of the variation of the barrier position.

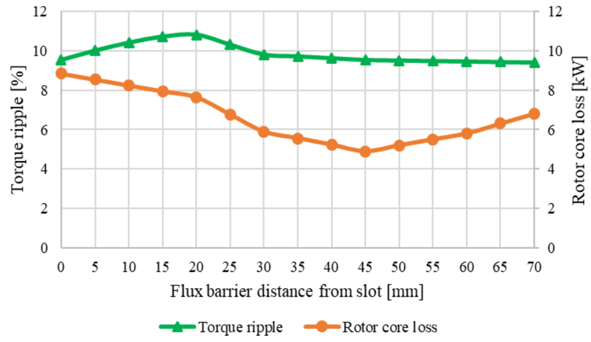

Fig. 9. Effect of the 5 mm flux barrier position on the torque ripple and rotor core losses.

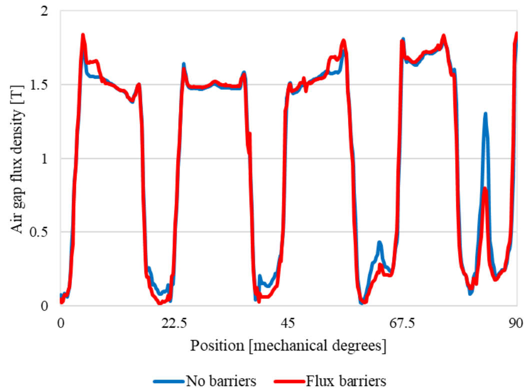

Fig. 10. Air gap flux density without and with flux barriers.

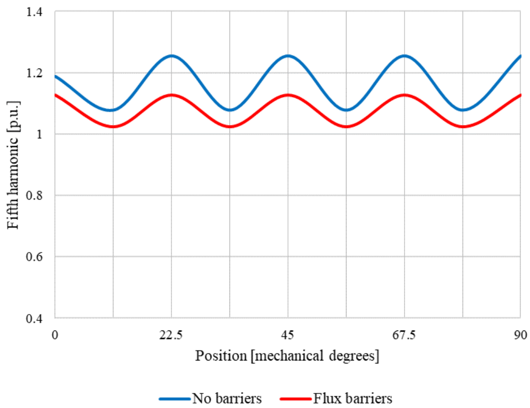

Fig. 11. Fifth harmonic of the air gap flux density without and with flux barriers.

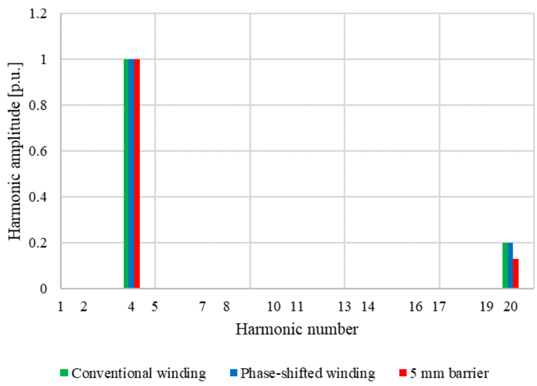

Fig. 12. Harmonic spectrum of the air gap flux density with no phase current and rated field current.

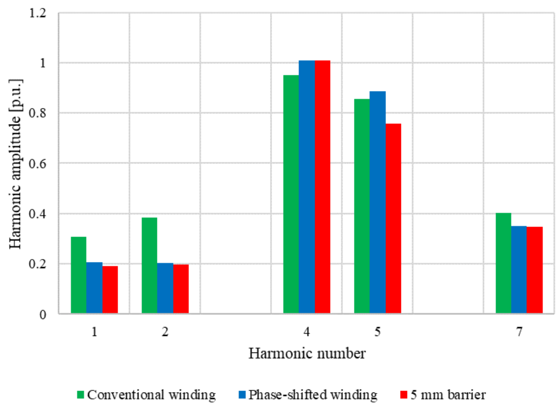

Fig. 13. Harmonic spectrum of the air gap flux density with phase current and no field current.

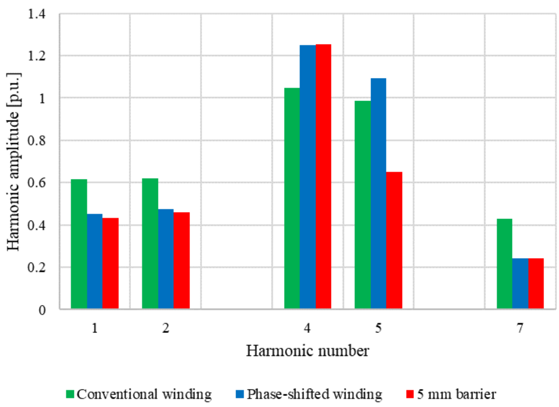

Fig. 14. Harmonic spectrum of the air gap flux density with rated phase current and rated field current.

B. *Rotor Core Flux Density Variation*

It is necessary to determine the effect of the flux barriers on the flux density within the rotor core. The focus is around the rotor teeth and the flux barriers. A layout of the different measurement positions of the flux densities in the rotor tooth and yoke is given in Fig. 15. The measurement positions indicated are used for the model with and without barriers in the yoke. Position A is used for a radial measurement, while positions B to D are all tangential flux densities.

The resultant flux density waveforms for the different specified positions are displayed in Figs. 16 to 19. The results at positions A and C show little change between the two models. The greatest difference is seen in Figs. 17 and 19. The flux density is increased at position B when the barriers are placed in the model, while at position D a strong decrease is seen between the waveforms. The latter indicates that the flux barrier prevents flux from penetrating further into the rotor core and channels it back towards the tooth. This explains why the rotor core losses are much lower when the barriers are added to the model.

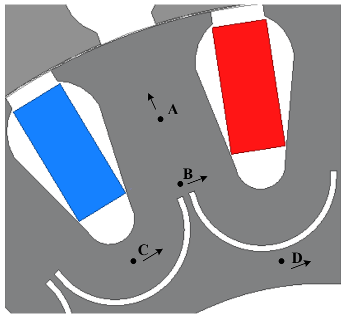

Fig. 15. Layout of positions for flux density comparison.

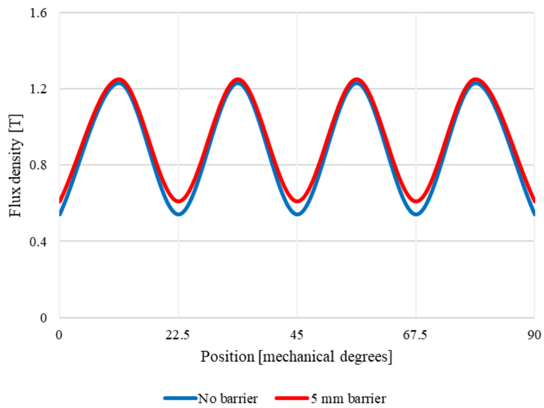

Fig. 16. Radial flux density without and with flux barriers at position A.

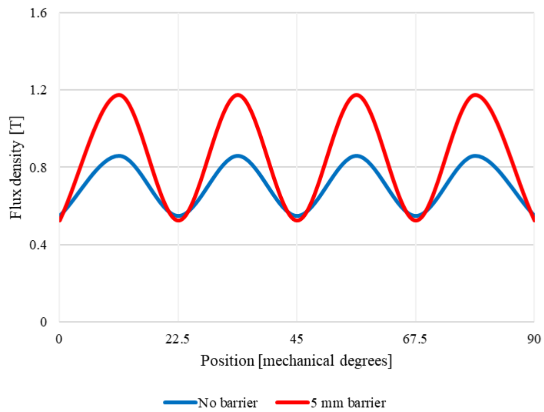

Fig. 17. Tangential flux density without and with flux barriers at position B.

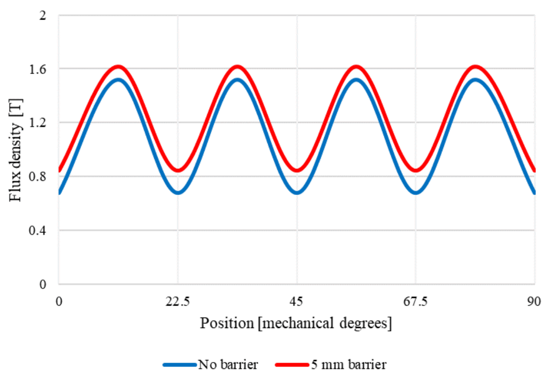

Fig. 18. Tangential flux density without and with flux barriers at position C.

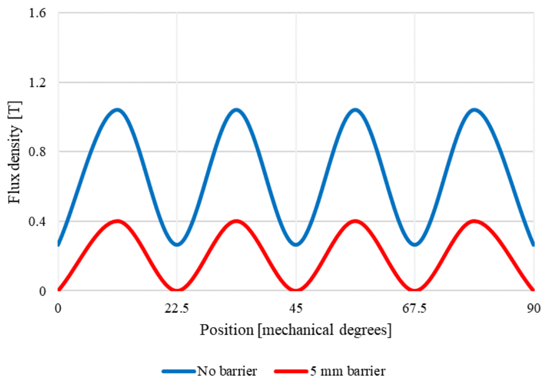

Fig. 19. Tangential flux density without and with flux barriers at position D.

V. Effect of Saturation

In Fig. 20, the effect of saturation by varying the rotor field current is shown on the rotor core losses without and with yoke flux barriers. The stator current was maintained at rated current. The dotted line indicates the rated field operating point of the machine and shows that the core is not yet in saturation. If the field current is increased to the point that the rotor core begins to deeply saturate, then the rotor core losses become a minimum and there is little difference between using yoke barriers or not. The latter, however, is at the expense of higher copper losses as seen in Fig. 21. Fig. 21 also displays the summation of the rotor core and copper losses as a function of the field current. As a matter of interest, the effect of saturation by varying the field current is repeated with no phase current present in the stator winding and the results between the model without and with yoke flux barriers are displayed in Fig. 22. The reduction of rotor core losses is also eminent in this scenario.

VI. Rotor Yoke Reduction Strategy

This strategy investigates the effect of the rotor yoke thickness on the rotor core loss and the machine performance. The approach is two-fold: (i) the rotor yoke thickness is varied and (ii) a non-uniform rotor yoke is applied by varying the inner rotor diameter in the shape of the flux barriers.

Fig. 23 illustrates the rotor yoke thickness in question. The rotor yoke is varied from 10 to 90 mm. The effect of this variation on the machine performance is displayed in Fig. 24 and Fig. 25. As expected, a reduced rotor yoke thickness results in lower core losses, but also sharply worsens the machine performance and torque ripple. A thickness of 45 mm is approximately equivalent to the location of the 5 mm flux barriers, and is chosen as one of the yoke designs.

Fig. 26 depicts the non-uniform rotor yoke applied to the design at the same point where the flux barriers are observed to be the most effective. A summary of the performance results of the three rotor yoke designs are provided in Table III. The non-uniform rotor yoke performs better than the uniformly reduced rotor yoke, but both strategies fall short when compared to the placement of the flux barriers in the rotor yoke.

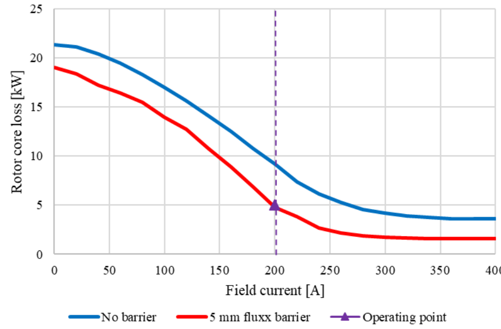

Fig. 20. Rotor core losses with rated phase current versus field current.

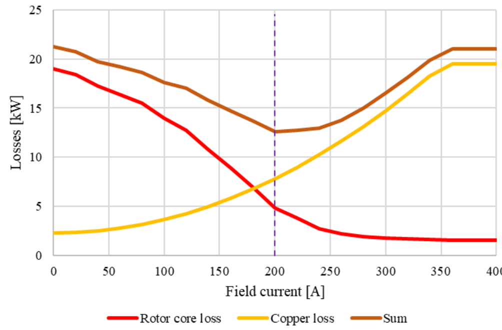

Fig. 21. Rotor core and copper losses versus field current.

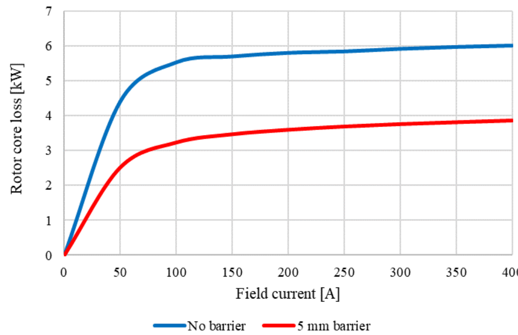

Fig. 22. Rotor core losses versus field current with no stator current.

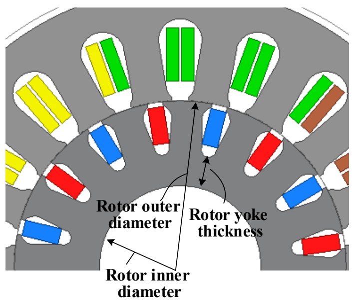

Fig. 23. Illustration of rotor yoke height.

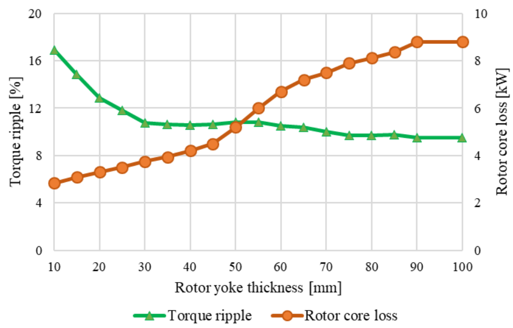

Fig. 24. Torque ripple and rotor core losses versus rotor yoke height.

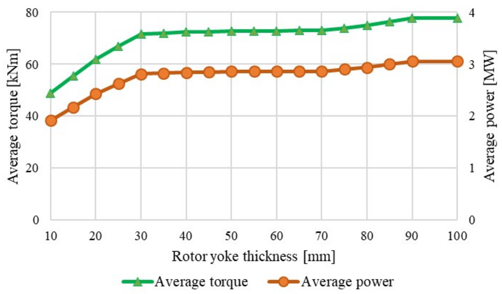

Fig. 25. Average torque and power versus rotor yoke height.

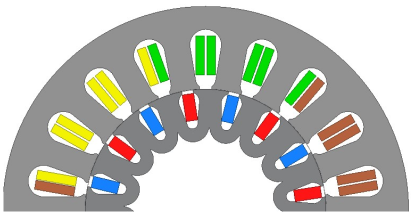

Fig. 26. Non-uniform rotor yoke.

TABLE III: PERFORMANCE OUTPUT OF ROTOR YOKE DESIGN STRATEGIES.

Performance parameter	Flux barrier	45 mm rotor yoke	Non-uniform rotor yoke
Power [MW]	3.05	2.85	2.9
Average torque [kNm]	77.58	72.61	73.8
Torque ripple [%]	9.53	10.6	10.05
Rotor core loss [kW]	4.9	4.32	4.20
Efficiency [%]	97.67	97.5	97.6

VII. CONCLUSION

In this paper, the effect of the rotor yoke design on specifically the rotor core losses, but also on the torque ripple and average torque of the machine, is investigated in a large non-overlap winding WRSM. The study reveals that placing flux barriers in the inner core of a large rotor yoke largely reduces the rotor core losses without affecting the machine performance negatively. The latter is only true for optimum values of barrier thickness and barrier position.

It is shown that deep saturation of the rotor core minimises the rotor core losses at rated stator current. Furthermore, in the case of deep saturation, little difference is found in the rotor core loss whether using rotor yoke flux barriers or not. However, with the core unsaturated (i.e. with zero to rated field current), the use of yoke flux barriers shows to be constantly effective.

It is found that a vast reduction in the rotor yoke height resulted in much lower rotor core losses, but with increased torque ripple and lower average torque. The non-uniform rotor yoke design yielded a better but similar outcome. Hence, considering the three yoke design strategies, the use of yoke flux barriers is found overall to be the best in the design of the rotor yoke.

VIII. REFERENCES

[1] J. Pyrhönen, T. Jokinen and V. Hrabovcová, *Design of Rotating Electric Machines*, Second edition, Wiley (United Kingdom), p. 201, 2014.

[2] G. Dajaku, S. Spas, X. Dajaku, D. Gerling, "An Improved Fractional Slot Concentrated Winding for Low-Poles Induction Machines", 19th *International Conference for Electrical Machines* (ICEM), Germany, September 2016, pp. 116-121.

[3] K. S. Garner and M. J. Kamper, "Reducing MMF harmonics and core loss effect of non-overlap winding wound rotor synchronous machine (WRSM)," *IEEE Energy Conversion* Congress and Exposition (ECCE), Cincinnati, OH, 2017, pp. 1850-1856.

[4] M. Barcaro, N. Bianchi and F. Magnussen, "Rotor flux–barrier geometry design to reduce iron losses in synchronous IPM motors under FW operations", *IEEE International Electrical Machines and Drives Conference* (IEMDC), Miami, FL USA, 2009.

[5] N. Bianchi, S. Bolognani, D. Bon and M. Dai Pre, "Rotor flux-barrier design for torque ripple reduction in synchronous reluctance and PM-assisted synchronous reluctance motors", *IEEE Transactions on Industry Applications*, Vol. 45, No. 5, pp. 921-928, May - June 2009.

[6] Magnetic materials - part 1-1: classification, International Standard IEC 60404-1:2000.

[7] C. L. Xia, L. Y. Guo, Z. Zhang, T. N. Shi and H. M. Wang, "Optimal Designing of Permanent Magnet Cavity to Reduce Iron Loss of Interior Permanent Magnet Machine", *IEEE Transactions on Magnetics*, Vol. 51, 2015.

[8] C. C. Hwang, C. M. Chang and C. T. Liu, "A fuzzy-based taguchi method for multi-objective design of PM motors", *IEEE Transactions on Magnetics*, Vol. 49, pp. 2153 – 2156, 2013.

[9] Z. Q. Zhu, D. Wu and W. Q. Chu, "Influence of local magnetic saturation on iron losses in interior permanent magnet machines", *International Conference on Electrical Machines (ICEM)*, Lausanne, Switzerland, 2016, pp. 1822 – 1827.

[10] Z.Q. Zhu and D. Wu, "On-load voltage distortion in fractional-slot interior permanent magnet machines", *IEEE Transactions on Magnetics*, Vol. 51, pp. 1 – 9, 2015.

[11] K. Yamazaki, Y. Kato, T. Ikemi and S. Ohki, "Reduction of Rotor Losses in Multilayer Interior Permanent-Magnet Synchronous Motors by Introducing Novel Topology of Rotor Flux Barriers", *IEEE Transactions on Industry Applications*, Vol. 50, No. 5, pp. 3185 – 3193, 2014.

[12] A. Dziechciarz and C. Martis, "New Shape of Rotor Flux Barriers in Synchronous Reluctance Machines Based on Zhukovski Curves", *9th International Symposium on Advanced Topics in Electrical Engineering*, Bucharest, Romania, pp. 221 – 224, 2015.

IX. BIOGRAPHIES

Karen S. Garner was born in Cape Town, South Africa on October 17, 1985. She completed the B. Eng degree in Electrical and Electronic Engineering at Stellenbosch University in 2007 and the M. Eng degree in Electrical Engineering at North-West University in 2015. She worked as an electrical engineer in the petrochemical industry from 2008 to 2016, completing multi-billion dollar projects from concept to construction. She is now working as a lecturer at Stellenbosch University and pursuing her PhD. She is registered as a Professional Engineer in South Africa and is supported by the South African National Research Foundation. Her research interests are novel electric machines, renewable energy and power transmission.

Maarten J. Kamper (SM'08) received the M.Sc (Eng.) degree in 1987 and Ph.D degree in 1996, from Stellenbosch University, Stellenbosch, South Africa. He has been with the academic staff of the Department of Electrical and Electronic Engineering, University of Stellenbosch, since 1989, where he is currently a Professor of electrical machines and drives. His research interests include computer–aided design and control of reluctance, permanent magnet, and induction machine drives. Prof. Kamper is a South African National Research Foundation (NRF) supported scientist and a Registered Professional Engineer in South Africa.